COMPARISON OF FRACTAL DIMENSION ALGORITHMS FOR THE COMPUTATION OF EEG BIOMARKERS FOR DEMENTIA

C Goh B Hamadicharef G T Henderson E C Ifeachor

University of Plymouth, U.K.

ABSTRACT

Analysis of the Fractal Dimension of the EEG appears to be a good approach for the computation of biomarkers for dementia. Several Fractal Dimension algorithms have been used in the EEG analysis of cognitive and sleep disorders. The aim of this paper is to find an accurate Fractal Dimension algorithm that can be applied to the EEG for computing reliable biomarkers, specifically, for the assessment of dementia. To achieve this, some of the common methods for estimating the Fractal Dimension of the EEG are reviewed and compared using serial EEG recordings of normal and subjects with dementia. Biomarkers computed from the Fractal Dimensions are assessed according to their ability to perform early detection, differential diagnosis of dementia and in identifying effects of channel variations in subjects with dementia. The initial findings have shown that not all Fractal Dimension algorithms are suitable for computation of EEG biomarkers for dementia. Typically, biomarkers obtained from the Zero Set and the Adapted Box algorithms have shown good discriminating power in the early detection and differential diagnosis of dementia. Two channels, namely P3 and PZ have also been singled out as the most affected channels in dementing subjects. This bodes well with recent neuroimaging findings which indicate that the posterior cortex is one of the main sites of cortical atrophy in early Alzheimer's Disease.

Keywords:

Fractal Dimension, factal dimension algorithms, EEG, dementia, biomarkers

INTRODUCTION

Improved life expectancy due to better lifestyle and nutrition has led to a significant increase in the number of people in the high-risk age groups that will develop neurological diseases such as dementia, Whitehouse (1). There is at present no cure for this cognitive disorder, although several acetylcholinesterase inhibitors such as galanthamine and donepezil have been registered in several countries for the mild symptomatic relief of dementia of the Alzheimer's type (DAT). Nonetheless, unless sufferers are diagnosed in the early stages, they cannot reap the maximum benefit of the treatments that may extend the time before significant mental decline occurs, Anand (2).

Several indices or “biomarkers” such as those obtained from neuroimaging, electrophysiology, biochemistryand genomics, Jelic (3) could benefit the early detection, diagnosis and prognosis of dementia. These markers, each having their own advantages and disadvantages, could be used complementarily to improve and provide a more well-informed diagnosis.

Currently, neuroimaging biomarkers produced from imaging techniques such as functional neuroimaging (fMRI) and positron emission tomography (PET) are amongst the most popular due to their high accuracies. Nonetheless, these markers are expensive to obtain and their interpretations are dependent on specialists' expertise. Therefore, they are less viable for use in the detection of the large at-risk population since ideally, everyone in the group would need to be tested at regular periods.

Electrophysiological biomarkers such as those observed from the human Electroencephalogram (EEG) offer the potential for providing an acceptable and affordable method in the routine screening of dementia in the early stages. The EEG is a record of the electrical activities of the brain. Due to its non-invasiveness and real-time depiction of brain activities, it has become an attractive tool in clinical practices with applications including the detection of seizure and epilepsy and brain tumours, Binnie et al (4). Research have revealed that the EEG could be a potential candidate for the early detection and differential diagnosis of dementia, Ktonas (5), Rosén (6). However, the complex and nonstationary characteristics of the EEG make automating the analysis process a challenging task.

Along with other nonlinear methods, the Fractal Dimension (FD) has been frequently used in the analysis of biomedical signals exhibiting non-stationary and transient characteristics such as the EEG, Pradhan and Dutt (7). It is potentially a good indicator of possible dementia because it is a measure of signal complexity and the complexity of the EEG of demented subjects has been shown to be generally lower than that of normals, Henderson (8). At present, a number of FD algorithms have been used in the analysis of EEG for cognitive disorders such as epilepsy, Esteller et al (9) and sleep disorders, Dvir et al (10).

The focus of this paper is to compare and assess the performance of FD algorithms for the computation of EEG biomarkers, specifically for the assessment of dementia. The goal is to find a FD algorithm that can

yield accurate biomarkers which capture the pathological changes in the EEG of subjects with dementia. By tracking the evolution of the biomarkers, clinicians and carers would be able to answer questions concerning the condition of the subject and offer the appropriate treatment options.

We report our findings based on the comparison of six common FD algorithms when applied to serial EEG recordings of healthy control subjects and those with dementia. The FDs obtained from each algorithm is combined into a single-valued index (biomarker). The FD algorithms are compared based on their ability to produce biomarkers that can clearly and accurately distinguished between normal and demented subjects. The performance of each algorithm is assessed using a metric (Method of Evaluation Metric) developed in our previous study, Henderson et al (11). From the results obtained, FD algorithms, which are suitable for the computation of EEG biomarkers for dementia are identified. These results are in good agreement with those obtained from imaging techniques, suggesting that the EEG could be used as a complementary measure to neuroimaging. More importantly, the results demonstrate how the automated analysis of EEG may contribute to objective measurements and provide affordable first-line of screening for dementia.

The paper is organised as follow. We begin by giving an overview of the FD of the EEG. Following this, a description of each of the FD algorithms investigated in this paper is given. We then describe the data used and how the biomarkers are obtained from the FDs computed by each algorithm. Subsequently, the FD algorithms are compared, analysed and evaluated. This is followed by a discussion on the results and findings of the paper. Finally, some concluding remarks and future directions of this study are given.

FRACTAL DIMENSIONS OF THE EEG

The term fractal relates to shapes and objects in space or fluctuations in time that possess a form of self-similarity whose dimension cannot be described by an integer value, Klonowski (12). A fractal object can be divided into identical or statistically exact copies and each copy can be made to match the whole object by shifting and stretching.

When thinking of the dimensions of an object, one is accustomed to associate it with the "topological dimension" (TD). For instance, a line has a TD of 1, a square 2 and a cube 3. This can be expressed in terms of the object's length as length^1, length^2 and length^3 for a line, square and cube respectively, where the exponent is the dimension.

However, the TD is not suitable for measuring the dimensions of fractals. Instead, the Hausdorff dimension, which may be a non-integer value is used. Taking the EEG as an example, the FD can be obtained by dividing the signal into smaller similar sections of length, *m*. As illustrated in Figure 1, the suitability of the Hausdorff dimension over the TD becomes apparent when one tries to select a suitable length to divide the time series. Indeed, it is often difficult to gauge what is a suitable length for each subsection of the time series, ie. a large *m* (*m*2) may result in finer features being overlooked, while a small *m* (*m*1) may result in a infinite number of segments. In contrast to the TD, which is an integer, the use of fractional dimension, compensates for the details smaller than the chosen length of each subsections.

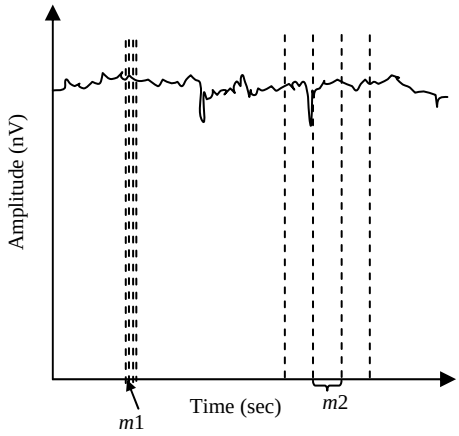

Figure 1. Dividing the EEG into subsection of length *m*.

Based on the self-similarity property of fractals, it is possible to to obtain the number of self-similar pieces forming the orignal signal by magnifying each subsection by a factor, *n*, and raising it to the power of the dimension, *D*. This is governed by the power law and can be expressed as :

$$S = n^D \tag{1}$$

The Hausdorff dimension, *D* can then be obtained as:

$$D = \ln(S) \Big/ \ln(n) \tag{2}$$

where *S* is the number of self-similar pieces and *n* is the magnification factor.

The FD thus measures the rate of addition of structural details with increased magnification, scale or resolution and therefore can be seen as a quantifier of complexity. FDs of the EEG computed in this manner will always be between 1 and 2 since it characterises the complexity of the signal under consideration on a 2-dimensional plane (voltage and time). For a signal with lower complexity, the FD is equal to 1 and for a more complex signal, *D* is close to 2.

A number of methods have been reported in the literature that are suitable for estimating the FDs of the

EEG, Esteller et al (9), Dvir et al (10), Petrosian (13). Here, 6 more common methods which have been demonstrated to estimate the FDs of the EEG with some success are compared.

FRACTAL DIMENSION ALGORITHMS

In the Katz's algorithm, Katz (14) the FD is obtained directly from the time series and can be defined as:

$$D = \frac{\log_{10}(L)}{\log_{10}(d)} \tag{3}$$

where L is the total length of the EEG time series and d is the distance (Euclidean) between the first point in the series and the point that provides the furthest distance with respect to the first point.

We see here that D is the Hausdorff dimension in equation 2 and by selecting the furthest distance, d, the algorithm uses the largest magnification to compute the FD. FDs computed in this manner are dependent on the units of measurement used. To resolve this, Katz proposed a normalisation as expressed below:

$$FD_{Katz\_norm} = \frac{\log_{10}(L/a)}{\log_{10}(d/a)} \tag{4}$$

where $\underline{a}$ is the average number of steps in the series.

Now, if we let, then Equation 4 can be written as:

$$FD_{Katz\_norm} = \frac{\log_{10}(n)}{\log_{10}\left(d/L\right) + \log_{10}(n)} \tag{5}$$

Petrosian's Algorithm

Petrosian's algorithm, Petrosian (13) can be used to provide a fast computation of the FD of a signal by translating the series into a binary sequence. Several variations of the algorithm exist. These algorithms primarily differ in the way the binary sequence is created. In this paper, the Petrosian C and Petrosian D FD algorithms are used. In the former, consecutive samples in the time series are subtracted and the binary sequence is created based on the result of the subtraction. A '+1' or '-1' is assigned for every positive or negative result respectively. In the latter algorithm, the binary sequence is formed by assigning a '1' for every difference between consecutive samples in the time series that exceeds a standard deviation magnitude and a '0' is assigned otherwise. The FD is computed as:

$$FD_{Petrosian} = \frac{\log_{10} n}{\log_{10} n + \log_{10}\left(\frac{n}{n + 0.4N_{\Delta}}\right)} \tag{4}$$

where n is the length of the sequence and N_{Δ} is the number of sign changes in the binary sequence.

Sevcik's Algorithm

The Sevcik's algorithm, Sevcik (18) estimates the FD from a set of N values, y_i sampled from a waveform between time 0 and t_{max}. The waveform is subjected to a double linear transformation that maps it into a unit square. The normalised abscissa of the square is x_i^* and the normalised ordinate is y_i^*, both of them defined as:

$$x_i^* = \frac{x_i}{x_{\max}}$$

$$y_i^* = \frac{y_i - y_{\min}}{y_{\max} - y_{\min}} \tag{6}$$

where x_{max} is the maximum x_i and y_{min} and y_{max} are the minimum and maximum y_i. The FD of the waveform is then approximated as follows:

$$FD_{Sevcik} = 1 + \frac{\ln(L) + \ln(2)}{\ln(2N')} \tag{7}$$

where L is the length of the time series in the unit square and $N' = N$-1.

Adapted Box Dimension

The Adapted Box dimension, Henderson et al (11), Henderson et al (16), Henderson et al (17) can be estimated by dividing a time series of T durations into segments of length Δt. For each segment, the extent, which is the difference between the minimum and maximum duration is derived. The mean extent $E(\Delta t)$ is then computed for a range of Δt and the dimension is computed by finding the best fit to the following Equation:

$$A(\Delta t) = TE(\Delta t) \approx A_0 \Delta t^{2-D} \tag{7}$$

where T is the total duration of the series, E is the mean extent, Δt is the segment length and D is the estimated FD.

Zero Set Dimension

To compute the dimension of the Zero Set, we form the set of instances when the record intersects with a suitable straight line. In this paper, the 0 V reference is used, whereby the TD of this set is 0, Henderson (17). The FD of this Zero set is computed by covering it with N line segments of length Δt and finding the best fit to Equation 8 below:

$$L(\Delta t) = tN(\Delta t) \approx L_0 \Delta t^{1-D} \quad (8)$$

where N is the total number of line segments, Δt is the segment length and D is the estimated FD.

DATA

The EEG recordings were obtained using the traditional 10-20 system, in conjunction with a strict protocol, Jasper (18). The common average montage (using the average of all channels as the reference) was used in all recordings. For all data, the recorded sampling rate was 256 Hz, which was further reduced to 128 Hz for analysis by averaging sets of two consecutive samples (for storage reasons). The EEG recordings encompassed various states: awake, hyperventilation, drowsy and alert with periods of eyes closed and open. To prevent electrical artefacts, which commonly occurs at the beginning of a record, and to give a standard four minutes of data to analyse, data from 60 s to 300 s from each record was used. This segment of data including artefacts was analysed and with no á priori selection of elements 'suitable for analysis'. This approach leads to a prediction of the usefulness of the algorithms, as they would most conveniently be used in practice.

EEGs were collected from seven patients (three AD patients, three mixed type - AD and multi-infarct dementia (MID) patients and one MID patient) and eight age matched controls (over 65 years of age), one young male and one young female. All of the age-matched controls and the two young volunteers had normal EEGs (confirmed by a Consultant Clinical Neurophysiologist). One age matched control (known as 'Vol1') has subsequently developed AD. This record is of particular interest because it is potentially of a subject early in transition from 'normal' to AD.

COMPUTATION OF BIOMARKERS FROM FRACTAL DIMENSIONS

Combining Estimated FDs into a Single Index

For each subject, the FDs computed by each algorithm are combined to form a single index (FD_{index}) or biomarker. A reliable biomarker will be able to differentiate clearly between a normal and demented subject.

To compute this index, the EEG data are divided into segments of 1s interval and the FD from each segment is plotted on a histogram. The mode of the histogram is taken as the composite measure of the FD. By doing so, we seek to find the FD that has the highest density for all twenty-one channels of EEG recordings Henderson (19). The index is derived using equation 9 below:

$$FD_{index} = \frac{\sum_{i=1}^{N} D_i^n FD_i}{\sum_{i=1}^{N} D_i^n} \quad (9)$$

where D_i is the histogram height (density) at FD FD_i and N is the total number of FDs. n is a control constant. When n = 1, the FD becomes the mean and when n tends to infinity, it tends to the mode. In this paper, n = 4 is chosen.

Figure 2 shows the distribution of the FD computed using the Sevcik algorithm for a normal subject (Vol7), an AD patient (AD2) and a mixed dementia (Mix1) patient. From this, a clear difference is seen in the FD distribution between the three subjects. In contrast to Vol7, the distribution of Mix1 tends towards lower FDs and AD2 has the lowest FD distribution as indicated by the FD_{index}s.

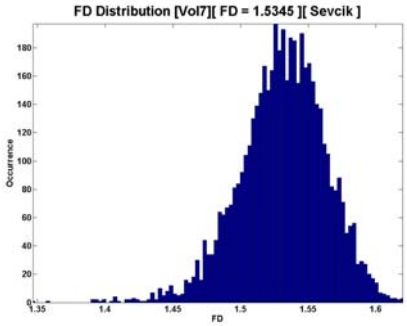

(a)

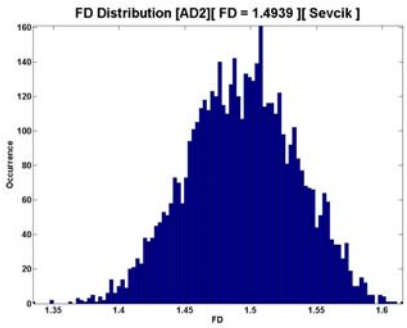

(b)

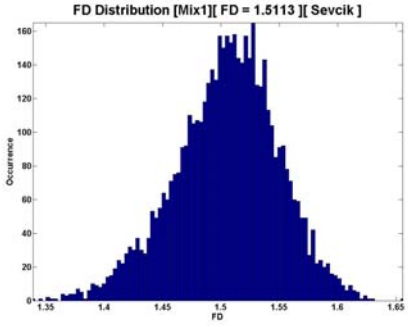

(c)

Figure 2. FD distribution of Vol7, AD2 and Mix1 estimated by Sevick algorithm.

Evaluation Metric

As this study seeks to compare and find a FD algorithm for the computation of biomarkers, it is important to have measures that describe how well the algorithms are performing in terms of the accuracy of the biomarkers in detecting the onset of dementia and differentiating between normal and demented subjects. Using the Jarque-Bera normality test, Judge et al (20), it has been shown that the FDs have a normal distribution. Hence, we have chosen to measure the performance of each algorithm using the Method Evaluation Metric (MEM), which we have developed in Henderson (11). The steps of the evaluation metric can be summarised as follow:

(i) Compute the candidate indices of all demented and control subjects using equation 9.

(ii) Compute mean μ and estimated population standard deviation (σ) of the index for control subjects.

(iii) Compute the difference (x) between the μ and the closest index from any of the demented subjects (ie. closest to normal).

(iv) Divide x computed in (iii) by the σ. In this way, the MEM describes how many σ the "most normal" demented subject is from the mean of the control subjects. In general, a higher MEM is more preferable and as a guide, a measure of 3σ is good, Henderson (20).

RESULTS AND DISCUSSIONS

The FDs algorithms presented earlier are used to compute biomarkers from every EEG recordings in our data set. It should be highlighted that for both data sets, Vol1 has been excluded from the computation of the MEM. This is because the subject went on to develop AD after the recording was taken and it is deemed that the accuracy of the MEM would be compromise if he/she had been included.

From the results in Figure 3, it can be deduced that the FD_{index} computed from the Adapted Box and Zero Set dimensions for both raw and auto-correlation of the EEG are more consistent than that produced by the other algorithms. In constrast to the latter algorithms, the biomarkers produced by the former are generally lower for demented subjects and higher for normal ones. This is apparent from the indices and MEMs (raw and auto-correlation of the EEG) presented in Table 1, Table 2 and Figure 4 respectively. The FD_{index} obtained from the raw EEG of the most normal demented subject for the Zero Set and Adapted Box dimension is 7.712σ and 4.69σ away from the normals respectively. The negative MEMs for the rest of the algorithms are due to the most normal demented subject having a higher FD_{index} than the mean FD_{index} of the normal subjects. These further confirmed the inconsistencies in the indices produced by these algorithms.

From the normalised FD_{index}s presented in Figure 3, it is clear that the Zero Set and Adapted Box dimensions have better discriminating power between normal and demented subjects over the other algorithms. These observations are in good agreement with the results of the t-test presented in Tables 3 and 4, which showed that the Zero Set and the Adapted Box dimensions are significantly more effective in separating normals from demented subjects ($p<0.001$) than the other algorithms and therefore are more promising for use in the early detection of dementia. Furthermore, they are able to clearly differentiate between the conditions of subjects within each group, with the Zero Set achieving better discriminations in the demented group ($p<0.001$) and the Adapted Box performing better in the group of normals ($p<0.001$).

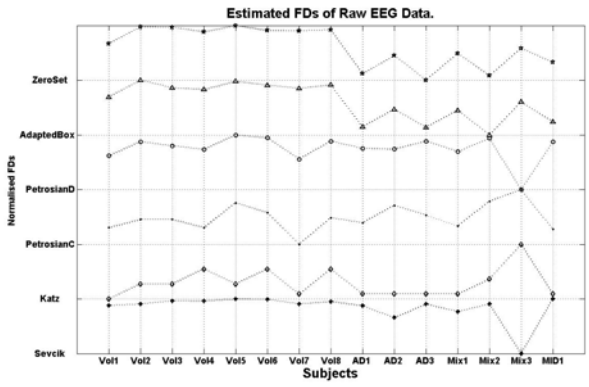

(a) Estimated FDs - Raw EEG.

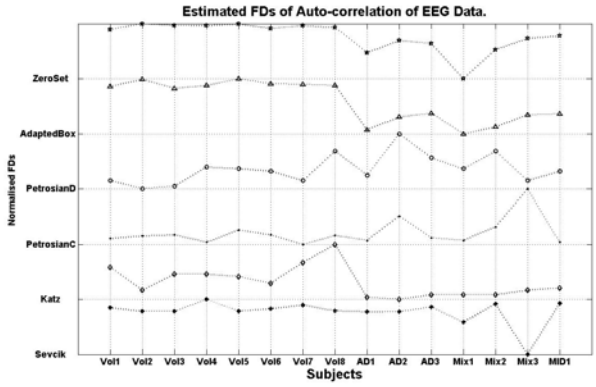

(b) Estimated FDs - Auto-correlation of EEG.

Figure 3. Comparison of FD algorithms applied to raw and auto-correlation of EEG.

In the case of the Petrosian C and Petrosian D algorithms, it is difficult to distinguish between the normal and demented groups by solely looking at the indices. These algorithms are highly dependent on the binary sequence used. The disadvantage of the Petrosian C method is that it does not take into account the magnitude of the slope sign variation when constructing the binary sequence. Hence, given a noisy signal, the algorithm may misinterpret signal variabilities due to noise as normal signal variations and include them in

the computation of the biomarkers. For the Petrosian D algorithm, poor discrimination could result from comparing the samples to a threshold and assigning 1s and 0 s according to the deviation from the threshold value. This may result in any intermediate values indicating the states between normal and dementing subjects not being capture accurately, thereby affecting the accuracy of the biomarkers computed. Similarly, the indices computed by the Sevcik algorithm are ambiguous. With the exception of Vol4, all normal subjects have lower FD_{index}s than Mix2 and MID1. It is therefore difficult to accurately pinpoint the conditions of particular subjects based on these indices and that the suitability of the algorithm in the computation of EEG biomarkers is questionable.

Amongst all the algorithms compared, the Katz algorithm presented the worst performance with a MEM of -3.5 as shown in Figure 4. Its poor discriminative power can be attributed to exponential transformation of the FDs. From equation 1, it is clear that the FD is sensitive to the initial offering of the stepsize (n) in the series. The FD will be fixed at 1 as n approaches infinity. Therefore, the biomarkers obtained from the algorithm may not be sufficiently pronounced to provide a clear distinction between normal and dementing subjects. The relatively low $\sigma_{control}$ also indicates that the computed biomarkers exhibit little variations between subjects and are therefore less appropriate for use in differential diagnosis. Indeed, it can be seen from the results that, as compared to the other algorithms, most of the control subjects have the same FD_{index} of 1.0002. Furthermore, the FD_{index}s s of the demented group show that it is hard to differentiate between a subject with AD from one with mixed dementia. These results have demonstrated that not all FD algorithms used for analysing the EEG are suitable for computation of EEG biomarkers for dementia.

In Esteller et al (9), it was reported that the Katz algorithm produced the most consistent results in terms of discrimination between states of brain functions when applied to 16 epileptic EEG recordings. Specifically, the results showed that it is effective in discriminating between the period before an epileptic seizure and the seizure period. The authors also showed that when tested on synthetic data, the Katz algorithm emphasised higher FDs and is relatively insensitive to noise. This leads us to believe that the algorithm is more efficient in detecting sharp/rapid signal changes like in epileptic seizures rather than the smaller, slower and more gradual changes in dementia.

Another interesting observation about the FD algorithms can be drawn from the respective FD_{index}s of Vol1. Since the subject subsequently developed AD after the EEG recording, his/her FD_{index} would be expected to be between that of a normal and a demented subject. Using this as a yardstick, only the Adapted Box and the Zero Set dimension manage to produce biomarkers that clearly indicate this difference as shown in the normalised FD_{index} in Figure 3. Based on these results, it is thus clear that the Adapted Box and the Zero Set dimensions are more suitable for the computation of EEG biomarkers for dementia.

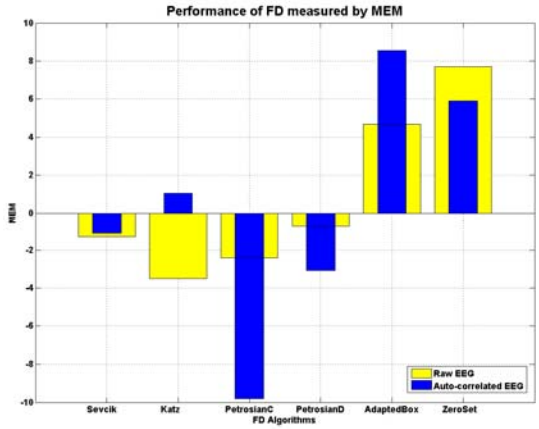

Figure 4. Performance of FD algorithms measured by MEM.

In Figure 5, the absolute value of the MEM of every channel for all FD algorithms are computed using both raw and autocorrelation of the EEG data. Here, we seek to compare the effectiveness of these algorithms in detecting which EEG channels are most affected and hence are better at determining the presence of dementia. It can be seen that although each algorithm presented different channels of significance, channels P3 and PZ has the most distinct change in the MEMs. This is an important finding as it concurs with a recent Magnetic Resonance Imaging (MRI) study, Fox et al (21), which showed that the main sites of cortical atrophy in early AD are in the medial temporal lobe (which is deep within the brain and not normally observable within surface EEG) and posterior cortex as indicated by channels P3 and PZ identified by the algorithms. Additionally, an interesting point to note is that channel PZ was identified by algorithms with poor discriminating power (Katz, Sevcik, Petrosian C and Petrosian D), while channel P3 by the Adapted Box and Zero Set algorithms. This suggests that those algorithms that are inferior in early detection and differential diagnosis may be useful in detecting dementia by monitoring the MEM variations per channel. More data need to be used to verify this finding. Nonetheless, the results suggest that the Zero Set and Adapted Box FD algorithms could be implemented in tools for the affordable first-line screening of patients with probable dementia prior to costly imaging examinations.

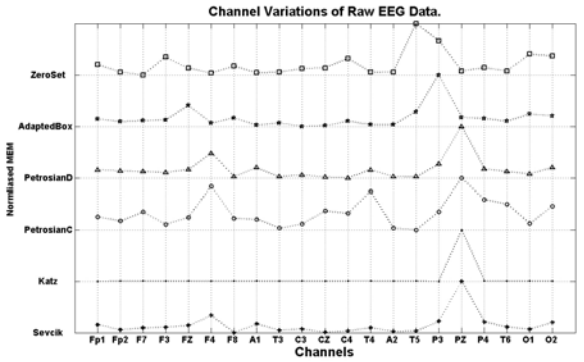

(a) Channel Variations - Raw EEG.

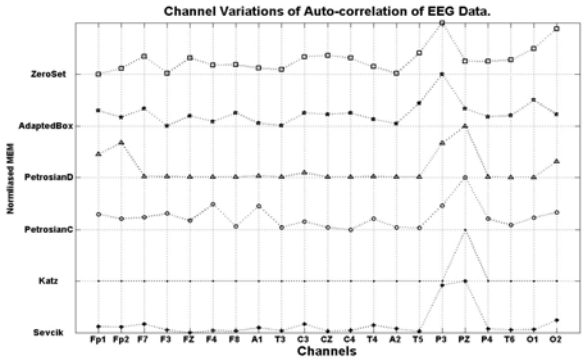

(b) Channel Variations – Auto-correlation of EEG.

Figure 5. Performance of FD algorithms based on channel variations of raw and auto-correlation of EEG.

TABLE 1 – Comparison of estimated FDs of raw EEG data (21 Channels).

Controls	Sevcik	Katz	Petrosian C	Petrosian D	Adapted Box	Zero Set
Vol1	1.5302	1.0001	1.0402	1.0183	1.2827	0.6466
Vol2	1.5344	1.0004	1.0412	1.0217	1.3361	0.7022
Vol3	1.5440	1.0004	1.0412	1.0207	1.3121	0.7011
Vol4	1.5431	1.0007	1.0402	1.0198	1.3063	0.6846
Vol5	1.5491	1.0004	1.0432	1.0233	1.3328	0.7065
Vol6	1.5485	1.0007	1.0420	1.0226	1.3201	0.6898
Vol7	1.5345	1.0002	1.0382	1.0175	1.3102	0.6888
Vol8	1.5416	1.0007	1.0414	1.0218	1.3213	0.6923
$\mu_{control}$	1.5422	1.0005	1.0411	1.0211	1.3198	0.6950
$\sigma_{control}$	0.0059	0.0002	0.0016	0.0019	0.0113	0.0082
Patients	**Sevcik**	**Katz**	**Petrosian C**	**Petrosian D**	**Adapted Box**	**Zero Set**
AD1	1.5293	1.0002	1.0408	1.0201	1.1877	0.5479
AD2	1.4934	1.0002	1.0429	1.0199	1.2429	0.6074
AD3	1.5340	1.0002	1.0417	1.0218	1.1857	0.5262
MIX1	1.5109	1.0002	1.0404	1.0193	1.2397	0.6149
MIX2	1.5346	1.0005	1.0434	1.0225	1.1618	0.5409
MIX3	1.3838	1.0012	1.0448	1.0102	1.2667	0.6319
MID1	1.5498	1.0002	1.0400	1.0216	1.2030	0.5851
MEM	-1.2839	-3.5000	-2.4046	-0.7412	4.6889	7.7120

TABLE 2 – Comparison of estimated FDs of auto-correlation of EEG data (21 Channels).

Controls	Sevcik	Katz	Petrosian C	Petrosian D	Adapted Box	Zero Set
Vol1	1.4516	1.0015	1.0274	1.0070	1.2441	0.6427
Vol2	1.4447	1.0005	1.0280	1.0064	1.2739	0.6694
Vol3	1.4447	1.0012	1.0282	1.0066	1.2346	0.6823
Vol4	1.4676	1.0012	1.0266	1.0080	1.2475	0.6796
Vol5	1.4451	1.0011	1.0293	1.0079	1.2769	0.6956
Vol6	1.4494	1.0008	1.0282	1.0077	1.2555	0.6517
Vol7	1.4565	1.0017	1.0261	1.0070	1.2531	0.6799
Vol8	1.4455	1.0025	1.0281	1.0092	1.2480	0.6604
$\mu_{control}$	1.4504	1.0013	1.0278	1.0075	1.2556	0.6784
$\sigma_{control}$	0.0087	0.0007	0.0011	0.0010	0.0151	0.0173
Patients	**Sevcik**	**Katz**	**Petrosian C**	**Petrosian D**	**Adapted Box**	**Zero Set**
AD1	1.4437	1.0002	1.0270	1.0074	1.0556	0.4116
AD2	1.4440	1.0001	1.0324	1.0105	1.1098	0.5314
AD3	1.4528	1.0003	1.0276	1.0087	1.1268	0.5034
MIX1	1.4235	1.0003	1.0270	1.0079	1.0379	0.1532
MIX2	1.4591	1.0003	1.0300	1.0092	1.0678	0.4414
MIX3	1.3617	1.0005	1.0384	1.0070	1.1203	0.5513
MID1	1.4601	1.0006	1.0266	1.0077	1.1247	0.5766
MEM	-1.1072	1.0521	-9.8069	-3.0617	8.5604	5.8903

TABLE 3 – t-Test results in differentiation between normal and demented subjects (Raw EEG).

Method	Group				t	p-value
	Demented		Normal			
	μ	σ^2	μ	σ^2		
Katz	1.0004	0.0000	1.0005	0.0000	0.71	< 0.5
PetrosianC	1.0420	0.0000	1.0411	0.0024	0.06	< 0.5
PetrosianD	1.0193	0.0000	1.0211	0.0038	0.98	< 0.5
Sevcik	1.5051	0.0032	1.5422	0.0353	1.72	< 0.2
Adapted Box	1.2125	0.0014	1.3198	0.1285	7.19	<0.001
Zero Set	0.5792	0.0017	0.6950	0.0670	7.31	<0.001

TABLE 4 – t-Test results in differentiation between normal and demented subjects (Auto-correlation of EEG).

Method	Group				t	p-value
	Demented		Normal			
	μ	σ^2	μ	σ^2		
Katz	1.0003	0.0000	1.0013	0.0004	3.76	< 0.005
PetrosianC	1.0299	0.0000	1.0278	0.0012	1.23	< 0.5
PetrosianD	1.0083	0.0000	1.0075	0.0009	1.37	< 0.2
Sevcik	1.4350	0.0012	1.4505	0.0752	1.15	< 0.5
Adapted Box	1.0918	0.0014	1.2556	0.2265	10.84	<0.001
Zero Set	0.4527	0.0209	0.6784	0.2988	4.10	<0.001

CONCLUSIONS

In this paper, we have compared six FDs algorithms for the computation of biomarkers for dementia based on the human EEG. The results showed that the Zero Set and the Adapted Box algorithms are the most consistent when used in the early detection and differential diagnosis of dementia. The biomarkers obtained from Petrosian C, Petrosian D and Sevcik algorithms are ambiguous, in that they have poor discriminating power between normal and demented subjects. Despite its reported consistency in discriminating epileptic states from EEG, the Katz algorithm has the worst performance. The poor distribution of the biomarkers is also reflected in the MEM. Unlike epileptic EEGs, the EEGs of demented patients are more sensitive to the FD algorithms used. In terms of the channel variations, all the algorithms compared performed relatively well. The algorithms have identified channels namely P3 and PZ as the most affected channels. The results, which are in good agreement with recent findings in imaging studies, suggest that monitoring the MEM variations in these channels could increase the discriminating power in the differential diagnosis of dementia. The results presented so far have raised interesting and challenging issues for both research and clinical areas of using EEG as a biomarker for dementia. Future work includes the use of a larger cohort and more diverse datasets.

REFERENCES

1. Whitehouse, P. J., 2003, The Lancet, 361– 1227

2. Anand, R., 1998, Clinician, 16, 14–22

3. Jelic, V., 1999, "Early diagnosis of Alzheimer's disease - Focus on quantitative EEG in relation to genetic, biochemical and neuroimaging markers", Ph.D. Thesis, Karolinska Institute, Sweden

4. Binnie, C. D., Copper, R., Mauguiere, F., Osselton, J. W., Prior, P. F., and Tedman, B. M., 2003, "Clinical Neurophysiology: EEG, Paediatric Neurophysiology, Special Techniques and Applications," Elsevier Science Publishing Company, UK

5. Ktonas, P. Y., 1997, CRC Critical Reviews in Biomedical Engineering, 9, 39–97

6. Rosén, I., 1996, Acta Neurologica Scandinavia, supplement 168, 63–70

7. Pradhan, N. and Dutt, D. N., 1993, Computers in Biology and Medicine, 23, 381–388

8. Henderson, A. R., 1997, Clinica Chimica Acta, 257, 25–40

9. Esteller, R., Vachtsevanos, G, Echauz, J, and B. Litt, 2001, IEEE Transactions on Circuitsand Systems I: Fundamental Theory and Applications, 48, 177–183

10. Dvir, I., Adler, Y., Freimark, D., and Lavie, P., 2002, American Journal Physiol Heart Circ Physiol, 283, 434–439

11. Henderson, G. T. , Wu, P., Ifeachor, E. C., and Wimalaratna, H. S. K., 1998, Proceedings of the 3rd International Conference on Neural Networks and Expert Systems in Medicine and Healthcare (NNESMED'98), 322–330

12. Klonowski, W., 2000, Machine and Vision, 9, 403-431

13. Petrosian, A, 1995, IEEE Symposium on Computer Based Medical Systems, 212–217

14. Katz, M., 1988, Comput. Biol. Med., 18, 145–156

15. Sevcik, C., 1998, Complexity International, 5

16. Henderson, G. T., Ifeachor, E. C., Wimalartna, H. S. K., Allen, E. M., and Hudson, N. R., 2000, First IEE International Conference on Advances in Medical Signal and Information Processing (MEDSIP'00), 284–289

17. Henderson, G. T., Ifeachor, E. C., Wimalartna, H. S. K., Allen, E. M., and Hudson, N. R., 2002, Proceedings of the 4th International Workshop on Biosignal Interpretation, Como, Italy, 319–322

18. Jasper, H. H., 1958, Electroencephalography and Clinical Neurophysiology, 10, 371–375

19. Henderson, G., Ifeachor, E. C., Hudson, N. R., and Wimalaratna, H. S. K., 2005, IEEE Transactions on Biomedical Engineering (Submitted)

20. Judge, G. G., Hill, R. C., Griffiths, W. E., Lutkepohl, H., and Lee, T. C., 1998, "Introduction to the Theory and Practice of Econometrics", Wiley, New York

21. Fox, N. C. and Rossor, M. N., 2001, IEEE Transactions on BiomedialEngineering, 358, 201–205